ChemComm

COMMUNICATION

View Article Online
View Journal | View Issue

Cite this: *Chem. Commun.*, 2021, 57, 639

Received 4th November 2020,
Accepted 27th November 2020

DOI: 10.1039/d0cc07269a

rsc.li/chemcomm

From silicates to oxonitridosilicates: improving optical anisotropy for phase-matching as ultraviolet nonlinear optical materials†

Xiaodong Zhang,[a] Lichao Guo,[a] Bingbing Zhang,*[a] Jin Yu,[a] Ying Wang,[a] Kui Wu,*[a] Hai-jun Wang[a] and Ming-Hsien Lee[b]

Oxonitridosilicates, in which O atoms in SiO_4 are partially substituted by N atoms, are proposed to improve optical anisotropies of silicates as UV NLO materials. The optical properties calculation showed that the heteroleptic SiO_xN_{4-x} (x = 1–3) tetrahedra have strong polarizability anisotropy and large hyperpolarizability. Accordingly, nine noncentrosymmetric (NCS) oxonitridosilicate crystals collected in the inorganic crystal structural database (ICSD) are evaluated by using the first principles method. Finally, Si_2N_2O and LiSiON are screened out owing to wide band gaps (6.49 and 6.95 eV), large birefringences (0.102 and 0.060 at 1064 nm), and large SHG coefficients (3.3 and 2.2 times that of d_{36}(KDP)). More importantly, the cation selection and structural characteristics that are beneficial for enhancing the band gap and birefringence are identified. This study provides a novel strategy to design and find UV NLO crystals.

Second harmonic generation (SHG) was observed for the first time in crystal quartz (α-SiO_2) by Franken *et al.* in 1961.[1] Although the discovery of this phenomenon marks the beginnings of nonlinear optics, quartz has not been widely used as a NLO material due to low frequency conversion efficiency.[2] Apart from the relatively small SHG coefficients (d_{11} = 0.30 pm V^{-1}),[3] another Achilles' heel for quartz crystals is the tiny birefringence that results in phase mismatch between fundamental and doubled frequency waves.[4,5] For similar reasons, silicates have not attracted much attention as NLO materials in which the SiO_4 tetrahedra are considered to be unfavorable to induce large birefringence.

In order to obtain crystals with strong SHG effects and sufficient birefringence, scientists tend to divert attention to other materials, such as perovskite, tungsten-bronze type crystals, iodates, phosphates, borates, carbonates, and chalcogenides.[6,7] Plenty of NLO materials have been found in these systems including KH_2PO_4 (KDP),[8] $LiNbO_3$ (LN),[9] β-BaB_2O_4 (BBO), LiB_3O_5 (LBO), and $KBe_2BO_3F_2$ (KBBF).[10] Meanwhile, for silicates, very few of them are studied as NLO materials although they have abundant number and diverse structures. $Rb_2Be_2Si_2O_7$ with a short absorption edge down to the vacuum UV was probed as a NLO material.[11–13] But the weak SHG coefficient and small birefringence block its further application. To enhance the SHG response as well as birefringence, transition metal cations with d^0 or d^{10} electronic configuration are introduced into silicates. $A^{II}_2TiOSi_2O_7$ (A^{II} = Ba or Sr)[14,15] and $Li_2A^I_4$ [$(TiO)Si_4O_{12}$] (A^I = K or Rb)[16] are found to have large SHG responses (4.5–8.0 × KDP). $Sr_2ZnSi_2O_7$ shows a SHG intensity that is 35 times that of α-SiO_2.[17] However, the introduction of transition metals causes a severe red-shift of the absorption edges, which hinders their application in the UV region. Another pathway to improve the NLO properties of silicates is combining SiO_4 groups with other building blocks with large energy gap, such as the BO_3, BO_4 and AlO_4 groups. $Ba_4(BO_3)_3(SiO_4)\cdot Ba_3X$ (X = Cl or Br),[18] $Cs_2B_4SiO_9$,[19] and Li_3AlSiO_5[20] have been synthesized guided by this strategy. These crystals achieve a balance between band gap and SHG response. However, all of their structures do not show structural characters for large birefringences.

In the latest research, heteroleptic polyhedra in which the positive ions are bonded to more than one anionic ligand forming mixed-anion groups are proposed and confirmed as superior functional building blocks (FBUs) for NLO materials.[21,22] Among them, heteroleptic tetrahedra BO_xF_{4-x} and PO_xF_{4-x} with large polarizability anisotropies have shown distinct advantages giving rise to birefringence and SHG coefficients.[23,24] Accordingly, a series of fluorooxoborates and fluorophosphates[23–32] were discovered as excellent deep-ultraviolet (DUV) NLO materials. As for the silicate series, the first inorganic fluorooxosilicophosphate $K_4Si_3P_2O_7F_{12}$

[a] *College of Chemistry and Environmental Science, Key Laboratory of Medicinal Chemistry and Molecular Diagnosis of the Ministry of Education, Chemical Biology Key Laboratory of Hebei Province, Hebei University, Baoding 071002, China. E-mail: zhangbb@hbu.edu.cn, wukui@hbu.edu.cn*

[b] *Department of Physics, Tamkang University, New Taipei City 25137, Taiwan*

† Electronic supplementary information (ESI) available: Calculated results of $(SiN_xO_{4-x})^{(4+x)-}$ (x = 0, 1, 2, 3, 4) anionic groups, the crystal structures of oxonitridosilicates, and electronic structures of Si_2N_2O and LiSiNO. See DOI: 10.1039/d0cc07269a

with an octahedral SiO_2F_4 group was synthesized by Pan's group.[33] However, it crystallizes in a centrosymmetric space group and as a result has no SHG effects. Very recently, the first noncentrosymmetric (NCS) fluorooxosilicophosphate $CsSiP_2O_7F$ with hexacoordinate SiO_5F species was synthesized by Zhao *et al.*[34] It shows an SHG intensity about 0.7 times that of KDP and is transparent in DUV. No inorganic fluorooxosilicate that contains SiO_xF_{4-x} tetrahedra has been reported yet. The strategy of introducing F to partially substitute O in SiO_4 or SiO_6 to improve birefringence has not been achieved.

Unlike fluorine, nitrogen atoms can more easily partially substitute oxygen atoms forming SiN_xO_{4-x} (x = 2 or 3) mixed-anion tetrahedra as found in oxonitridosilicates. The heteroleptic tetrahedra provide another way to make up for the limitations in birefringence of silicates. In this communication, the $(SiNO_3)^{5-}$, $(SiN_2O_2)^{6-}$, and $(SiN_3O)^{7-}$ groups with large polarizability anisotropy and high hyperpolarizability are identified as novel superior FBUs to enhance birefringence and simultaneously to generate a large SHG effect and short cutoff edge as UV NLO materials. Oxonitridosilicates are identified as new candidate systems to explore new UV NLO materials by a first principles study.

To evaluate the basic NLO-related properties of the $(SiN_xO_{4-x})^{(4+x)-}$ (x = 1–3) anionic groups, we firstly investigate their electronic structure and optical properties using density functional theory (DFT) calculations implemented in the Gaussian09 package[35] at the 6-31G level. As shown in Table S1 (ESI†), the polar $(SiNO_3)^{5-}$, $(SiN_2O_2)^{6-}$, and $(SiN_3O)^{7-}$ groups exhibit obvious polarizability anisotropy of 5.2, 9.0, and 4.8, respectively. As a comparison, the polarizability anisotropy of $(BO_3F)^{4-}$, $(BO_2F_2)^{3-}$ and $(BOF_3)^{2-}$ groups calculated by using the same method and parameters are 2.1, 3.4, and 2.5, respectively.[23] To visibly illustrate the polarizability anisotropy of SiO_xN_{4-x} groups, a polarizability anisotropy surface is defined and drawn. In two-dimensions, for example, the polarizability anisotropy curve is defined as the difference between the polarizability ellipsoid and the sphere with a radius determined by the minimum polarizability in the same direction as shown in Fig. 1(a) and (b). Accordingly, the polarizability anisotropy surfaces of the $(SiNO_3)^{5-}$, $(SiN_2O_2)^{6-}$, and $(SiN_3O)^{7-}$ groups are constructed and drawn with their structures in the same orientation as shown in Fig. 1(c) and (d). From the polarizability anisotropy configuration of $(SiN_xO_{4-x})^{(4+x)-}$ groups, one can find that the N^{3-} anion is easier to be polarized than the O^{2-} anion, which results in the obvious polarizability anisotropy of $(SiN_xO_{4-x})^{(4+x)-}$ groups. In addition, the heteroleptic $(SiN_xO_{4-x})^{(4+x)-}$ groups exhibit much larger hyperpolarizability than that of $(SiO_4)^{4-}$ and $(SiN_4)^{8-}$. It is worth noting that the substitution of O by N significantly reduced the HOMO–LUMO gap (HOMO, the highest occupied molecular orbital; LUMO, the lowest unoccupied molecular orbital). In oxonitridosilicate crystals, N atoms are coordinated with more than one Si atom, which will eliminate the non-bonding electrons and expand the band gap to achieve UV transmittance.

The NCS oxonitridosilicate crystals that contain $(SiN_xO_{4-x})^{(4+x)-}$ (x = 2 or 3) groups are searched from the Inorganic Crystal Structural Database (ICSD). In total, 9 crystals are obtained including Si_2N_2O,[36] LiSiON,[37] $CaSi_2O_2N_2$,[38] $BaSi_6N_8O$,[39] $Ba_3Si_6O_9N_4$,[40] $SrSiAl_2N_2O_3$,[41] $Ba(Al_2Si_3)N_4O_4$,[42] $Ba(AlSi_4)O_3N_5$,[42] and $Y_2Si_3O_3N_4$.[43,44] As shown in Fig. S1 (ESI†), these crystals show a plentiful structural diversity with different connection modes between $(SiN_xO_{4-x})^{(4+x)-}$ (x = 2–4) groups including two-dimensional layers and three-dimensional networks. Subsequently, the first-principles high-throughput screening pipeline for nonlinear optical materials (FHSP-NLO) method[45,46] is used to predict their band gaps, birefringences, and SHG coefficients. The CASTEP package[47] is employed to perform self-consistent field (SCF) calculation and structural relaxation with the norm-conserving pseudopotentials (NCP)[48–50] and GGA-PBE exchange–correction functional.[51] The OptaDOS code[52,53] is used to calculate linear optical properties. The formula proposed by Sipe[54] and developed by Lin and Lee *et al.*[55,56] is used to calculate second-order susceptibility $\chi^{(2)}$ tensors. The hybrid functionals based on screened Coulomb potential HSE[57,58] are used to obtain more accurate band gaps (E_g-HSE) by performing the DFT plane-wave code (PWmat) run on GPU machines.[59,60] The scissors operator is set as the difference between E_g-HSE and E_g-GGA and used to correct the SHG coefficients of the crystals. Other parameters are set as the same as our recently published works.[45,46]

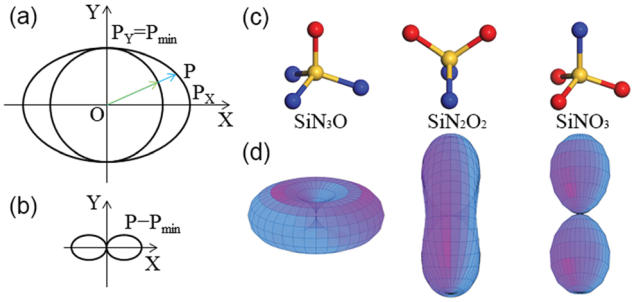

Fig. 1 (a) The two-dimensional diagram of the anisotropic polarizability and (b) the corresponding polarizability anisotropy curve (surface if three-dimension), which is defined as the difference between the polarizability ellipsoid and the sphere with a radius determined by the minimum polarizability in the same direction. (c) The representation of $(SiN_3O)^{7-}$, $(SiN_2O_2)^{6-}$, and $(SiNO_3)^{5-}$ groups and (d) their polarizability anisotropy surface.

The calculated results of the NCS oxonitridosilicates are listed in Table 1. For comparison, some silicates that are reported as promising ultraviolet NLO materials are selected and calculated under the same conditions as listed in Table S2 (ESI†). As shown in Table 1, the calculated band gaps of the oxonitridosilicates are widely dispersed. LiSiON and Si_2N_2O show very large band gaps (6.95 and 6.49 eV). This means that the transparency windows of the two crystals could extend to the DUV region (<200 nm). In contrast, trivalent rare-earth metal oxonitridosilicates $Y_2Si_3O_3N_4$ and the oxonitridosilicates containing Al atoms, *i.e.* $Ba(AlSi_4)O_3N_5$, $Ba(Al_2Si_3)N_4O_4$, and $SrSiAl_2N_2O_3$, exhibit relatively small band gaps ranging from 3.66 to 5.15 eV. Three alkaline-earth metal oxonitridosilicates, $CaSi_2O_2N_2$, $BaSi_6N_8O$, and $Ba_3Si_6O_9N_4$, show relatively large band gaps ranging from 5.41 to 5.82 eV. The N atoms are two- or three-coordinated with Si atoms in the above

Table 1 The chemical formula, ICSD collection numbers, space groups (SG), calculated band gaps both using GGA and HSE (E_g-GGA and E_g-HSE, units: eV), birefringences (Δn) at 1064 nm, and SHG coefficients ($\chi^{(2)}$) with scissors correction of selected oxonitridosilicates. Note the scissors operators that are used to correct $\chi^{(2)}$ are set as the difference between E_g-HSE and E_g-GGA

Formula	ICSD	SG	E_g-GGA	E_g-HSE	Δn	$\chi^{(2)}$ (pm V^{-1}) (+sci.)
Si_2N_2O	66539	$Cmc2_1$	5.23	6.49	0.102	$\chi_{113} = -1.615$; $\chi_{223} = -2.123$; $\chi_{333} = 2.557$
LiSiON	34106	$Pca2_1$	5.57	6.95	0.060	$\chi_{113} = 0.596$; $\chi_{223} = 1.710$; $\chi_{333} = -0.318$
$CaSi_2O_2N_2$	413882	$P2_1$	4.63	5.82	0.035	$\chi_{112} = -0.059$; $\chi_{123} = -0.028$; $\chi_{222} = 0.023$; $\chi_{233} = 0.034$
$BaSi_6N_8O$	415272	$Imm2$	4.33	5.62	0.015	$\chi_{113} = 0.162$; $\chi_{223} = -1.921$; $\chi_{333} = 6.827$
$Ba_3Si_6O_9N_4$	259431	$P3$	4.51	5.41	0.010	$\chi_{111} = 0.998$; $\chi_{222} = 0.853$; $\chi_{113} = -0.041$; $\chi_{333} = 0.746$
$SrSiAl_2N_2O_3$	408170	$P2_12_12_1$	4.17	5.15	0.015	$\chi_{123} = -2.360$
$Ba(Al_2Si_3)N_4O_4$	194213	$A2_1am$	3.58	4.50	0.042	$\chi_{111} = 1.494$; $\chi_{122} = -0.008$; $\chi_{133} = -3.336$
$Ba(AlSi_4)O_3N_5$	194212	$A2_1am$	3.17	3.66	0.073	$\chi_{111} = -0.001$; $\chi_{122} = 1.294$; $\chi_{133} = -0.194$
$Y_2Si_3O_3N_4$	89931	$P\bar{4}2_1m$	3.13	4.01	0.005	$\chi_{123} = -4.970$

oxonitridosilicates. To investigate the effects of different coordination types of N atoms on the band gaps, the distribution of electrons on them are analyzed. In $BaSi_6N_8O$, N(1) atoms are two-coordinated while N(2) and N(3) are three-coordinated with Si atoms. The partial density of states (PDOS) of three N atoms shows that the non-bonding 2p orbitals of three-coordinated N atoms are obviously eliminated in the top of the valence bands (TVB) compared with two-coordinated N atoms (Fig. S2(a), ESI†). In $Y_2Si_3O_3N_4$, all N atoms are two-coordinated with Si atoms. As shown in Fig. S2(b) (ESI†), two-coordinated N atoms contribute more electrons at the TVB than that of bridge and terminal O atoms and result in a small band gap (4.01 eV). Through the above analysis, one can find that cations and the coordination types of N atoms are the two crucial factors that determine the band gap. Alkali metal cations Li^+ or even no cations are beneficial for large band gaps, while Al^{3+} cations are disadvantageous. In addition, N atoms are better to be three-coordinated with Si atoms to eliminate their non-bonding 2p orbitals as much as possible.

As to the birefringence, oxonitridosilicates showed a significant improvement compared with that of silicates as shown in Fig. 2. The results demonstrate that oxonitridosilicates can break through the restriction on birefringence in silicates and induce sufficient optical anisotropy for achieving phase-matching during SHG. Among the studied oxonitridosilicates, Si_2N_2O and LiSiON have both large birefringences and wide band gaps. In the two crystals, the SiN_3O tetrahedra linked each other by N atoms forming $[Ge_2O_2N_2]^{2-}$ layers. The polarizability maximum plane of the SiN_3O tetrahedra of them are schematically drawn as circle planes with the crystal structure in Fig. S1 (ESI†). Their polarizbility maximum planes are nearly coplanar arranged. This would generate the maximum polarizbility in the layers and minimum porlarizbility perpendicular to the layers. As a result, the structures would induce strong optical anisotropy. Besides the structural arrangement, a high number density of anisotropic polarized anionic groups is another factor that is beneficial for obtaining large birefringence.[61] Compared with Si_2N_2O, the insertion of Li^+ cations reduces the number density of SiN_3O tetrahedra and accordingly decreases the birefringence. As the number density of the SiN_3O groups decreases, another crystal $CaSi_2O_2N_2$ that also contains $[Ge_2O_2N_2]^{2-}$ layers shows a smaller birefringence of

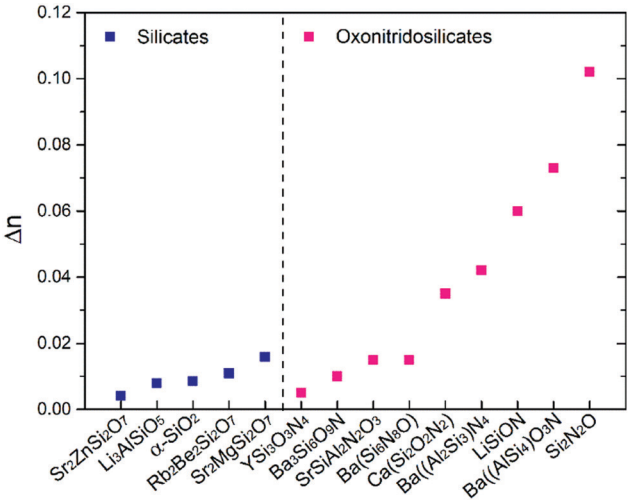

Fig. 2 The calculated birefringence of selected silicates and oxonitridosilicates.

0.035 at 1064 nm. Disordered orientation or/and low number density of $(SiN_xO_{4-x})^{(4+x)-}$ groups in $BaSi_6N_8O$, $Ba_3Si_6O_9N_4$, $SrSiAl_2N_2O_3$, and $Y_2Si_3O_3N_4$ result in them having small birefringences.

Most of the studied oxonitridosilicates have large SHG coefficients ($>2 \times d_{36}$(KDP)). $BaSi_6N_8O$ has the largest SHG coefficient of 6.827 pm V^{-1} ($8.8 \times d_{36}$(KDP)) among them. The SHG coefficients of Si_2N_2O and LiSiON are 3.3 and 2.2 times that of d_{36}(KDP), respectively. The results reveal that the $(SiN_xO_{4-x})^{(4+x)-}$ (x = 2 and 3) are excellent FBUs to generate strong SHG effects. Considering all the three properties, Si_2N_2O and LiSiON are the two best candidates of ultraviolet NLO materials. More discussions about the two crystals are listed in the ESI.† For the calculated results of Si_2N_2O and LiSiON one can also refer to ref. 62.

In summary, oxonitridosilicates are proposed as promising ultraviolet NLO materials. The $(SiN_xO_{4-x})^{(4+x)-}$ (x = 1–3) anionic groups exhibit strong polarizability anisotropy and large hyperpolarizability that are expected to produce large birefringence and SHG coefficient in oxonitridosilicate crystals. Therefore, 9 NCS oxonitridosilicate crystals that contain $(SiN_xO_{4-x})^{(4+x)-}$ (x = 2 and 3) groups are evaluated by using the DFT method. The results show that oxonitridosilicates can significantly

improve birefringences as well as SHG coefficients compared with silicates. Besides, the 2p dangling bonds of N atoms can be maximally eleminated through being three-coordinated with Si atoms and accordingly widen the band gap into the deep-ultraviolet (DUV) region (<200 nm). Finally, Si_2N_2O and LiSiON are screened out due to wide band gaps (6.49 and 6.95 eV), large birefringences (0.102 and 0.060 at 1064 nm), and SHG coefficients (3.3 and 2.2 times that of d_{36}(KDP)). This study provides a novel strategy to design and find ultraviolet NLO crystals.

This work was supported by the National Natural Science Foundation of China (Grant No. 5207021329, 51702356, 21975062, and 51872324), the Natural Science Foundation of Hebei Province (Grant No. B2019201433, E2020201005, and E2019201049), and the Advanced Talents Incubation Program of the Hebei University (Grant No. 521000981279).

Conflicts of interest

There are no conflicts to declare.

References

1 P. A. Franken, A. E. Hill, C. W. Peters and G. Weinreich, *Phys. Rev. Lett.*, 1961, **7**, 118–119.
2 J. Jerphagnon and S. K. Kurtz, *Phys. Rev. B: Solid State*, 1970, **1**, 1739–1744.
3 K. Hagimoto and A. Mito, *Appl. Opt.*, 1995, **34**, 8276–8282.
4 G. Ghosh, *Opt. Commun.*, 1999, **163**, 95–102.
5 R. N. Smartt and W. H. Steel, *J. Opt. Soc. Am.*, 1959, **49**, 710.
6 G. Zou and K. M. Ok, *Chem. Sci.*, 2020, **11**, 5404–5409.
7 X. Dong, L. Huang, C. Hu, H. Zeng, Z. Lin, X. Wang, K. M. Ok and G. Zou, *Angew. Chem., Int. Ed.*, 2019, **58**, 6528–6534.
8 Y. S. Liu, W. B. Jones and J. P. Chernoch, *Appl. Phys. Lett.*, 1976, **29**, 32–34.
9 G. D. Boyd, R. C. Miller, K. Nassau, W. L. Bond and A. Savage, *Appl. Phys. Lett.*, 1964, **5**, 234–236.
10 C. Chen, T. Sasaki, R. Li, Y. Wu, Z. Lin, Y. Mori, Z. Hu, J. Wang, S. Uda, M. Yoshimura and Y. Kaneda, *Nonlinear Optical Borate Crystals*, Wiley-VCH Verlag GmbH & Co. KGaA, Weinheim, Germany, 2012.
11 R. A. Howie and A. R. West, *Nature*, 1976, **259**, 473.
12 Z. G. Hu, M. Yoshimura, Y. Mori and T. Sasaki, *J. Cryst. Growth*, 2005, **275**, 232–239.
13 R. A. Howie and A. R. West, *Acta Crystallogr., Sect. B: Struct. Crystallogr. Cryst. Chem.*, 1977, **33**, 381–385.
14 W. Zhao, F. Zhang, J. Liu, B. Hao, S. Pan, F. Zhang and L. Liu, *J. Cryst. Growth*, 2015, **413**, 46–50.
15 J. Yuan, P. Fu, J. Wang, F. Guo, Z. Yang and Y. Wu, *Prog. Cryst. Growth Charact. Mater.*, 2000, **40**, 103–106.
16 T. L. Chao, W. J. Chang, S. H. Wen, Y. Q. Lin, B. C. Chang and K. H. Lii, *J. Am. Chem. Soc.*, 2016, **138**, 9061–9064.
17 M. Mutailipu, Z. Li, M. Zhang, D. Hou, Z. Yang, B. Zhang, H. Wu and S. Pan, *Phys. Chem. Chem. Phys.*, 2016, **18**, 32931–32936.
18 X. Lin, F. Zhang, S. Pan, H. Yu, F. Zhang, X. Dong, S. Han, L. Dong, C. Bai and Z. Wang, *J. Mater. Chem. C*, 2014, **2**, 4257.
19 H. Wu, H. Yu, S. Pan, Z. Huang, Z. Yang, X. Su and K. R. Poeppelmeier, *Angew. Chem., Int. Ed.*, 2013, **52**, 3406–3410.
20 X. Chen, F. Zhang, L. Liu, B.-H. Lei, X. Dong, Z. Yang, H. Li and S. Pan, *Phys. Chem. Chem. Phys.*, 2016, **18**, 4362–4369.
21 H. Kageyama, K. Hayashi, K. Maeda, J. P. Attfield, Z. Hiroi, J. M. Rondinelli and K. R. Poeppelmeier, *Nat. Commun.*, 2018, **9**, 772.
22 J. K. Harada, N. Charles, K. R. Poeppelmeier and J. M. Rondinelli, *Adv. Mater.*, 2019, **31**, 1805295.
23 B. Zhang, G. Shi, Z. Yang, F. Zhang and S. Pan, *Angew. Chem., Int. Ed.*, 2017, **56**, 3916–3919.
24 B. Zhang, G. Han, Y. Wang, X. Chen, Z. Yang and S. Pan, *Chem. Mater.*, 2018, **30**, 5397–5403.
25 G. Shi, Y. Wang, F. Zhang, B. Zhang, Z. Yang, X. Hou, S. Pan and K. R. Poeppelmeier, *J. Am. Chem. Soc.*, 2017, **139**, 10645–10648.
26 X. Wang, Y. Wang, B. Zhang, F. Zhang, Z. Yang and S. Pan, *Angew. Chem., Int. Ed.*, 2017, **56**, 14119–14123.
27 Y. Wang, B. Zhang, Z. Yang and S. Pan, *Angew. Chem., Int. Ed.*, 2018, **57**, 2150–2154.
28 Z. Zhang, Y. Wang, B. Zhang, Z. Yang and S. Pan, *Angew. Chem., Int. Ed.*, 2018, **57**, 6577–6581.
29 Z. Zhang, Y. Wang, B. Zhang, Z. Yang and S. Pan, *Inorg. Chem.*, 2018, **57**, 4820–4823.
30 M. Luo, F. Liang, Y. Song, D. Zhao, F. Xu, N. Ye and Z. Lin, *J. Am. Chem. Soc.*, 2018, **140**, 3884–3887.
31 M. Mutailipu, M. Zhang, B. Zhang, L. Wang, Z. Yang, X. Zhou and S. Pan, *Angew. Chem., Int. Ed.*, 2018, **57**, 6095–6099.
32 L. Xiong, J. Chen, J. Lu, C. Pan and L. Wu, *Chem. Mater.*, 2018, **30**, 7823–7830.
33 G. Han, B. Lei, Z. Yang, Y. Wang and S. Pan, *Angew. Chem., Int. Ed.*, 2018, **57**, 9828–9832.
34 Q. Ding, X. Liu, S. Zhao, Y. Wang, Y. Li, L. Li, S. Liu, Z. Lin, M. Hong and J. Luo, *J. Am. Chem. Soc.*, 2020, **142**, 6472–6476.
35 M. J. Frisch, *et al.*, *Gaussian09, Revision D.01*, Gaussian, Inc., Wallingford CT, 2009.
36 J. Sjöberg, G. Helgesson and I. Idrestedt, *Acta Crystallogr., Sect. C: Cryst. Struct. Commun.*, 1991, **47**, 2438–2441.
37 Y. Laurent, J. Guyader and G. Roult, *Acta Crystallogr., Sect. B: Struct. Crystallogr. Cryst. Chem.*, 1981, **37**, 911–913.
38 H. A. Höppe, F. Stadler, O. Oeckler and W. Schnick, *Angew. Chem., Int. Ed.*, 2004, **43**, 5540–5542.
39 F. Stadler, R. Kraut, O. Oeckler, S. Schmid and W. Schnick, *Z. Anorg. Allg. Chem.*, 2005, **631**, 1773–1778.
40 H. W. Wei, X. M. Wang, H. Jiao and X. P. Jing, *J. Alloys Compd.*, 2017, **726**, 22–29.
41 R. Lauterbach and W. Schnick, *Z. Anorg. Allg. Chem.*, 1998, **624**, 1154–1158.
42 W. B. Park, S. P. Singh and K. S. Sohn, *J. Am. Chem. Soc.*, 2014, **136**, 2363–2373.
43 P. L. Wang, P. E. Werner, L. Gao, R. K. Harris and D. P. Thompson, *J. Mater. Chem.*, 1997, **7**, 2127–2130.
44 C. M. Fang, G. A. De Wijs, R. A. De Groot, R. Metselaar, H. T. Hintzen and G. De With, *Chem. Mater.*, 2000, **12**, 1071–1075.
45 B. Zhang, X. Zhang, J. Yu, Y. Wang, K. Wu and M.-H. Lee, *Chem. Mater.*, 2020, **32**, 6772–6779.
46 J. Yu, B. Zhang, X. Zhang, Y. Wang, K. Wu and M.-H. Lee, *ACS Appl. Mater. Interfaces*, 2020, **12**, 45023–45035.
47 S. J. Clark, M. D. Segall, C. J. Pickard, P. J. Hasnip, M. I. J. Probert, K. Refson and M. C. Payne, *Z. Kristallogr.*, 2005, **220**, 567–570.
48 M.-H. Lee, PhD thesis, The University of Cambridge, 1996.
49 J. Lin, A. Qteish, M. Payne and V. Heine, *Phys. Rev. B: Condens. Matter Mater. Phys.*, 1993, **47**, 4174.
50 A. M. Rappe, K. M. Rabe, E. Kaxiras and J. D. Joannopoulos, *Phys. Rev. B: Condens. Matter Mater. Phys.*, 1990, **41**, 1227.
51 J. P. Perdew, K. Burke and M. Ernzerhof, *Phys. Rev. Lett.*, 1996, **77**, 3865–3868.
52 A. J. Morris, R. J. Nicholls, C. J. Pickard and J. R. Yates, *Comput. Phys. Commun.*, 2014, **185**, 1477–1485.
53 R. J. Nicholls, A. J. Morris, C. J. Pickard and J. R. Yates, *J. Phys.: Conf. Ser.*, 2012, **371**, 012062.
54 C. Aversa and J. E. Sipe, *Phys. Rev. B: Condens. Matter Mater. Phys.*, 1995, **52**, 14636–14645.
55 J. Lin, M.-H. Lee, Z.-P. Liu, C. Chen and C. J. Pickard, *Phys. Rev. B: Condens. Matter Mater. Phys.*, 1999, **60**, 13380–13389.
56 B. Zhang, M. Lee and Z. Yang, *Appl. Phys. Lett.*, 2015, **106**, 031906.
57 J. Heyd, G. E. Scuseria and M. Ernzerhof, *J. Chem. Phys.*, 2003, **118**, 8207–8215.
58 A. V. Krukau, O. A. Vydrov, A. F. Izmaylov and G. E. Scuseria, *J. Chem. Phys.*, 2006, **125**, 224106.
59 W. Jia, J. Fu, Z. Cao, L. Wang, X. Chi, W. Gao and L.-W. Wang, *J. Comput. Phys.*, 2013, **251**, 102–115.
60 W. Jia, Z. Cao, L. Wang, J. Fu, X. Chi, W. Gao and L.-W. Wang, *Comput. Phys. Commun.*, 2013, **184**, 9–18.
61 B. Zhang, E. Tikhonov, C. Xie, Z. Yang and S. Pan, *Angew. Chem., Int. Ed.*, 2019, **2**, 1–6.
62 L. Kang, G. He, X. Zhang, J. Li, Z. Lin and B. Huang, 2020, arXiv:2009.06932v1.

